Final Report: NIOSH Grant 5 R01 OH02858- (01- 03)

Computational Methods in Industrial Ventilation

Principal Investigator: Dr. Michael R. Flynn

University of North Carolina @ Chapel Hill

50272-101

REPORT DOCUMENTATION PAGE	1. REPORT NO.	2.	3. PB97-104400

4. Title and Subtitle Computational Methods in Industrial Ventilation	5. Report Date 1995/09/14
	6.
7. Author(s) Flynn, M. R.	8. Performing Organization Rept. No.
9. Performing Organization Name and Address Department of Environmental Sciences and Engineering, School of Public Health, University of North Carolina, Chapel Hill, North Carolina	10. Project/Task/Work Unit No.
	11. Contract (C) or Grant(G) No. (C) (G) R01-OH-02858
12. Sponsoring Organization Name and Address	13. Type of Report & Period Covered
	14.

15. Supplementary Notes

16. Abstract (Limit: 200 words)

An existing computer code was expanded to predict air flow patterns around workers and obstacles, to develop models of exposure from these flow fields, and to conduct flow visualization and tracer experiments using a mannequin and a wind tunnel in order to validate the computer predictions of exposure. The two dimensional discrete vortex method for the time dependent velocity field around an ellipse in a uniform free stream was successfully expanded to include multiple objects in the flow. The concept of numerical flow visualization was introduced as an analytical tool. A particle tracking algorithm was introduced into the code to predict the time dependent concentration field and integrate this field over various regions in both space and time providing exposure estimates when appropriate computational breathing zones are identified. The experimental examinations of velocity and concentration fields were in good agreement with the numerical predictions made. Enough of the primary contaminant transport mechanisms data was captured by the computer model to allow reasonable quantitative estimates of exposure for a static three dimensional experiment with a box and mannequin in the wind tunnel. The vortex method was able to capture the evolution of the particularly large scale eddies responsible for contaminant transport in the vicinity of workers.

17. Document Analysis a. Descriptors

b. Identifiers/Open-Ended Terms NIOSH-Publication, NIOSH-Grant, Grant-Number-R01-OH-02858, End-Date-06-30-1995, Control-technology, Indoor-air-pollution, Air-flow, Air-quality-control, Mathematical-models, Industrial-hygiene

c. COSATI Field/Group

18. Availability Statement	19. Security Class (This Report)	21. No. of Pages 51
	22. Security Class (This Page)	22. Price

(See ANSI-Z39.18) *See Instructions on Reverse* **OPTIONAL FORM 272(4-77)** (Formerly NTIS-35) Department of Commerce

TABLE OF CONTENTS

Abstract

This is the Final Performance Report for NIOSH Grant 5 R01 OH02858-(01-03), entitled "Computational Methods in Industrial Ventilation." It is presented as a list of publications with reprints, and a discussion of how these papers relate to the Specific Aims. At the time this report was submitted, the third publication entitled "Experimental and Numerical Studies on the Impact of Work Practices used to Control Exposures Occurring in Booth-type Hoods" was in press at the **American Industrial Hygiene Association Journal**. A brief summary of the results of this paper are found in this report in the section on Specific Aims and their Relationship to the Publications. In addition, a Masters thesis is included as an Appendix with the relevant experimental work.

List of Publications

Kim, T. and Flynn, M.R. "Numerical Simulation of Air Flow Around Multiple Objects Using the Discrete Vortex Method" **Journal of Wind Engineering and Industrial Aerodynamics**, 56(2,3):213-234, (1995).

Flynn, M.R., Chen, M., Kim, T. and Muthedath, P. "Computational Simulation of Worker Exposure Using a Particle Trajectory Method" **Annals of Occupational Hygiene**, 39(3):277-289, 1995.

Flynn, M.R., Lackey, B.D., and Muthedath, P. "Experimental and Numerical Studies on the Impact of Work Practices used to Control Exposures Occurring in Booth-Type Hoods" **American Industrial Hygiene Association Journal**, In Press.

Significant Findings

Positive Results

The major positive results may be summarized as follows: (1) The two-dimensional discrete vortex method for the time-dependent velocity field around an ellipse (the worker) in a uniform freestream has been successfully expanded to include multiple objects in the flow. Specifically, a square is added to represent a workpiece. This permits simulations of various work practices within large booth-type hoods to be examined, e.g., changing the position of the worker with respect to the flow direction. The concept of numerical flow visualization is introduced as an analysis tool much as a smoke tube is currently used as a field assessment tool. (2) A particle tracking algorithm is introduced into the code in order to predict the time-dependent concentration field and to integrate this field over various regions in both space and time. This provides exposure estimates when appropriate "computational breathing zones" are identified. The determination of these zones is associated with identifying the recirculation region downstream of the worker. (3) Experimental examinations of the velocity and concentration fields are in good agreement with the numerical predictions. The computer model captures enough of the primary contaminant transport mechanisms to allow reasonable quantitative estimates of exposure for a static three-dimensional experiment with a box and mannequin in a wind tunnel. Special techniques are used to account for contaminant transport in the plane perpendicular to the simulation plane which helps overcome some of the limitations inherent in two-dimensional simulations. The ability of the vortex method to capture the evolution of the velocity field in time, particularly large scale eddies responsible for contaminant transport in the vicinity of workers, is especially encouraging. The dynamic adaptivity of vortex methods is particularly efficient at the high Reynolds numbers of significance in problems concerning human exposure to airborne contaminants.

Negative Results

There were no major negative results, however several limitations were identified. One is the difficulty in specifying, a priori, the region of integration for determining the breathing zone concentration. The need for further research in this area is evident. Three-dimensional calculations should prove more realistic, although there are other factors such as variations in boundary conditions and source momentum which also must be considered. Efforts at developing a parallel processor version of the code were abandoned, and we relied heavily on the multipole expansion algorithm provided by Dr. Greengard. Methods continue to evolve for the rapid solution of N-body problems and these will undoubtedly improve the efficiency of vortex methods. However, the effort needed to develop the methods, in house, is not, at present, a worthwhile use of time. More pressing issues of how to address variations in boundary conditions, realistic source terms, and three-dimensional considerations are more deserving of research.

The continued use of vortex methods appears encouraging, however three-dimensional methods in complicated geometry are limited at present. Use of finite element and other types of computational fluid dynamic algorithms are needed for comparison. The actual method selected for solving the equations is probably less critical than determining the fluid phenomenon of importance and the sensitivity of solutions to changes or uncertainties in boundary conditions.

Utility of Findings

The algorithms and experimental results obtained here provide a basis for improved numerical models to estimate human exposure and optimize control solutions. Ultimately more complex and realistic simulations can be developed, but as a benchmark these solutions are valuable. In addition, the algorithms provide a way to conduct "numerical flow visualizations" for estimating the formation of reverse flow zones and the stagnant regions that may compromise the beneficial effect of a contemplated ventilation design. The most immediate application suggested by the research is for a worker with a hand-held source of contaminant working in a booth, or otherwise generally uniform flow, to orient themselves such that the air flow direction is primarily from the side not from the back. *These results are suggested for sources with negligible momentum, and may not be applicable to spray applications where strong jet-effects are involved.* This is an important area for further research, along with detailed field confirmation of results.

Specific Aims and Relationship to Publications

The Specific Aims of the original proposal were: (1) To expand an existing computer code to predict air flow patterns around a worker and nearby obstacle; (2) to develop models of exposure from these flow fields, and (3) to conduct flow visualization and tracer experiments with a mannequin and wind tunnel to validate the computer predictions of exposure. Each of these aims is addressed, in sequence, by the publications in the order listed. The original discrete vortex code was designed to model flow around a worker in a uniform freetream by representing the worker as a 2-dimensional elliptical cylinder. The publication entitled "Numerical Simulation of Air Flow Around Multiple Objects Using the Discrete Vortex Method" accomplishes specific aim (1) by expanding the algorithm to address not only a worker (ellipse) but workpiece (square). The code is flexible enough to allow different positions of the worker with respect to the object. At this point only the time-dependent velocity field is calculated.

The publication entitled "Computational Simulation of Worker Exposure Using a Particle Trajectory Method" uses the original vortex code and adds a solution procedure for predicting not only the concentration field but exposure as well. This concentration algorithm is validated with flow visualizations and tracer work with only the mannequin, i.e., no work object is present. This accomplished Specific Aim (2), and laid the foundation for extension to the situation with the workpiece present. This was accomplished in the publication entitled "Experimental and Numerical Studies on the Impact of Work Pratices used to Control Exposures Occurring in Booth-Type Hoods." Here the algorithm developed in specific aim (1) for the combined velocity field was integrated with the exposure algorithm developed in publication 2 and a complete flow visualization and tracer study was conducted to validate the predictions and complete Aim (3).

The third paper is "in-press" as of the date of submission of this report. Anticipated publication is sometime in mid-to-late 1996. A brief summary of the results of this third paper is given here. The primary objective was to combine the discrete-vortex air-velocity algorithm described in the paper "Numerical simulation of air flow around multiple objects using the discrete vortex method" with the concentration algorithm described in the paper entitled "Computational simulation of worker exposure using a particle trajectory method" The desire was conduct an experimental validation of numerical predictions of exposure for two different orientations of worker and object with respect to the freestream. These configurations and a sample velocity field for each are shown in Figures 15 and 16 of the first paper. Wind tunnel studies using a mannequin with "hand-held" source of sulfur hexafluoride tracer gas, and a square box as a workpiece were conducted. Mannequin-exposures were measured in the "breathing-zone" with an electron capture detector for both orientations. These exposures are shown in the graph below as a function of wind tunnel air speed for configurations A (back-to-flow) and B (side-to-flow). The Block designation (Blk 1,2) is simply a replicate run. The side-to-flow configuration is clearly superior for all velocities as indicated by the dramatically lower exposures.

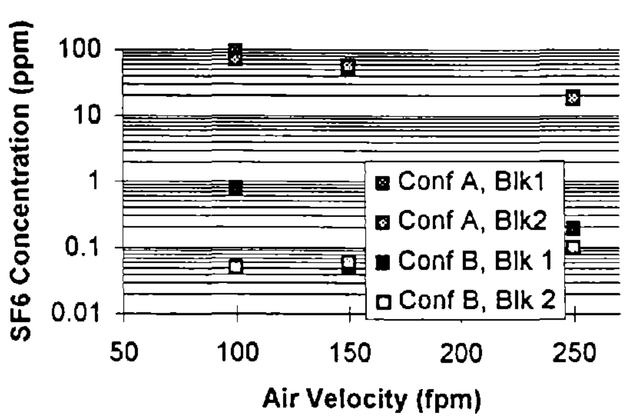

Numerical predictions of exposure depended upon correct identification of a region of space to integrate over, particularly for the side-to-flow case (config B). At 150 fpm the numerical prediction for exposure in Configuration A was 42 ppm and the measured value was 54 ppm. For the same velocity in Configuration B the prediction was 0.05 ppm, the measured value was 0.4 ppm.

The following flow-visualization photos are from the wind-tunnel work described above. They were obtained using the smoke-wire technique described previously in "Airflow Pattern Around a Worker in a Uniform Freestream" by Kim and Flynn, **AIHAJ** 52(7):287-296 (1991).

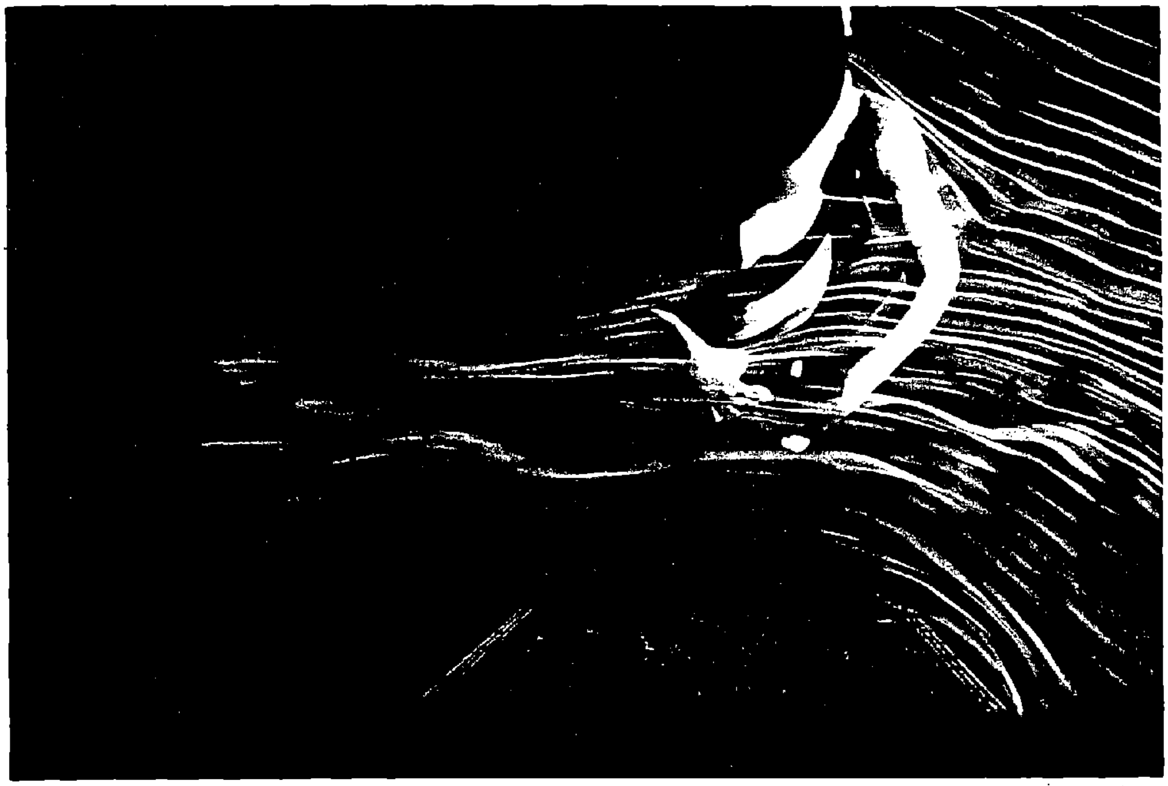

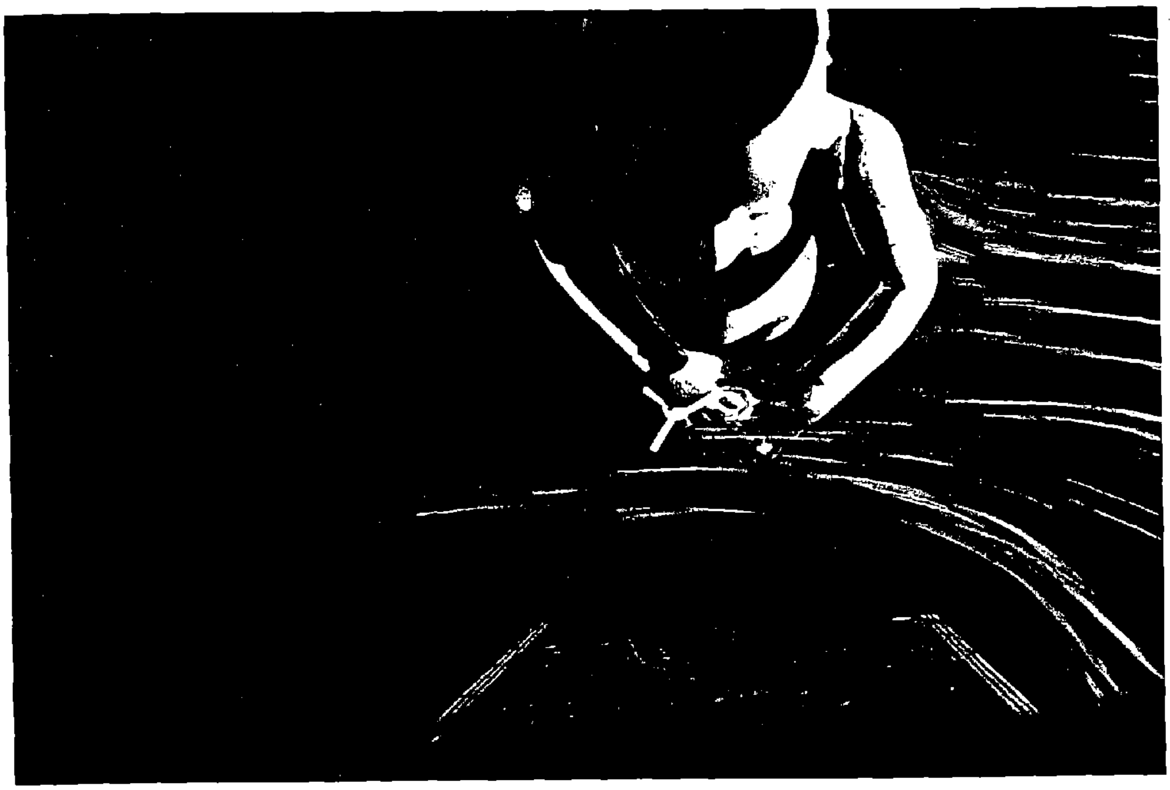

Air flow streamlines shown around mannequin and box for configuration B (side-to-flow) flow is from right-to-left. Top photo 150 fpm, bottom photo 250 fpm.

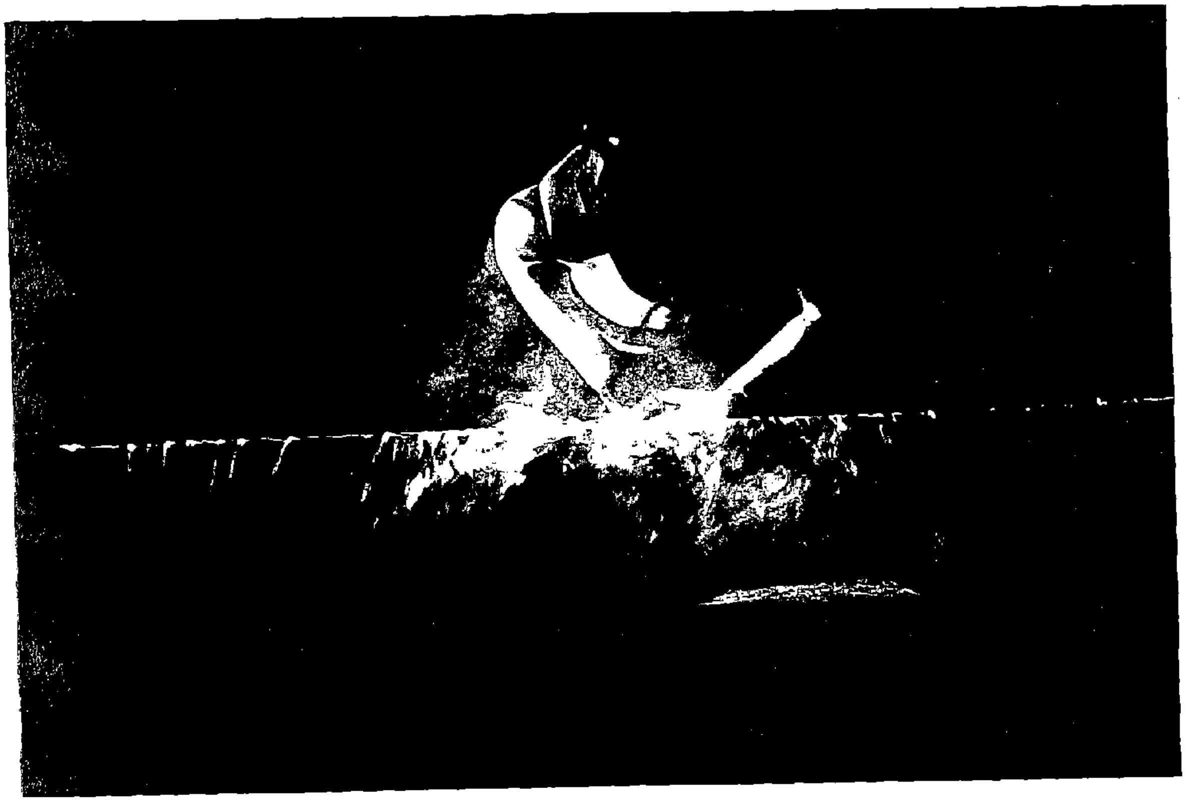

Configuration A (back-to-flow) at 250 fpm, top photo shows view from above, airflow is from top-to-bottom. Bottom photo is side view of same configuration flow from left-to-right. Box is downstream of mannequin in each case.

Appendix

Master's thesis of Brad Lackey

A Study of Worker Exposure from a Hand-Held Contaminant Source in a Simulated Spray Booth Operation

by

Bradley D. Lackey

A technical report submitted to the Faculty of the University of North Carolina at Chapel Hill in partial fulfillment of the requirements for the degree of Master of Science in Public Health in the Department of Environmental Science and Engineering.

Chapel Hill

August 1993

Approved by:

Michael R. Flynn, Sc.D.

Richard M. Kamens, M.S.P.H.

Lori A Todd, Ph.D.

TABLE OF CONTENTS

ACKNOWLEDGMENTS

I would like to thank my technical report advisor, Mike Flynn, for his guidance and patience. His suggestions and insight helped focus this work and made the entire process flow more smoothly than I could have hoped. It has been a pleasure to work with him.

Thank you to Kwangseog Ahn for his help in the lab, familiarizing me with the equipment, and for his advice in technical procedure. My experimental technique benefited from his direction.

I would like to thank the ARIH Faculty for the opportunity to study at UNC and fulfill my dream of attending graduate school. I enjoyed the courses they offer and regret having not taken more.

The academic and emotional support from the other students throughout the Department of Environmental Sciences and Engineering was remarkable. I feel fortunate to have formed friendships with so many exceptional people.

C.L. Lassiter deserves credit for his tenaciousness in keeping the student body informed of deadlines and the means of meeting them. His personal interest in the students shows in the quality of his work.

I would lastly like to thank my friend Gretchen Squires, whose enthusiasm inspired me to initiate the entire graduate school process.

LIST OF FIGURES

LIST OF TABLES

ABSTRACT

Tracer gas concentrations generated from a hand-held source are measured in the breathing zone of a mannequin, and for an elliptical cylinder positioned in a wind tunnel. Effects on breathing zone concentration due to worker position relative to the direction of airflow and a workpiece are examined. Flow visualization by the smoke wire technique is performed. Worker position was found to be statistically significant in breathing zone concentration. Positioning the worker with the air flow from the side results in a drop of roughly two to three orders of magnitude compared to positioning the worker with the airflow from the back. Interaction was noted between worker position and airflow rate. Tracer gas concentrations were lower in the breathing zone of the mannequin than for the cylinder. The placement of an object downstream of the worker when airflow is from the back resulted in a roughly two-fold increase in breathing zone tracer gas concentration when compared to predicted values with a worker only. Positioning a worker sideways to the airflow appears to result in a substantial decrease in contaminant exposure. Applications and limitations of the results are discussed.

INTRODUCTION

Local exhaust ventilation (LEV) is commonly used to reduce worker exposure to airborne contaminants to acceptable levels. LEV design has historically been based on achieving a proper capture velocity, using empirical equations based on hood airflow and distance between the source and the exhaust.[1]

When work generates contaminant over a large area, it is often necessary to enclose the entire operation to effectively capture the contaminant and prevent it from escaping into the general work environment. Large exhaust enclosures, such as walk-in spray booths, require a worker to be completely within the enclosure. Design of exhaust booths is based on airflow through the hood according to booth size, or ultimately to air speed through the booth. Recommended air speed varies depending on the type of contaminant and work being done.

Unfortunately, design parameters which effectively contain contaminant within the booth cannot predict how that system will protect the worker within the booth from exposure to the contaminant. Air currents which arise within the system disturb the hood-induced airflow and degrade the effectiveness of contaminant control. The most widely recognized sources of air motion are thermal effects and motion of machinery, materials, and worker within the hood.

Both the worker and the work piece within the booth become obstacles in the airstream and the free flow field within the booth is disturbed. It has been shown that the presence of an object (e.g. a person) in the flow field can create boundary layer separation, resulting in counterrotating eddies (vortices) downstream of the object.[2]

Researchers[3-6] note that as vortices form downstream of a bluff body in a free flow stream, the air mass within these vortex regions moves as a rigid body and is shed downstream. One author[4] states that in a room where contaminant is emitted into a vortex region, the average concentration within the vortex region may be ten times as high as in the air extracted by room ventilation.

This reverse flow region which develops immediately downstream of an object can carry contaminant from the point of release (downstream of the worker) back upstream and into the breathing zone. Thus, vortex formation is an important factor in worker exposure since it greatly interferes with the free field flow in the booth. By drawing contaminant back toward the breathing zone, vortex formation can undermine the intent of the local exhaust — which is to reduce worker exposure.

Studies performed to address these issues have revealed a better understanding of the problem, but have not been as successful in finding easy solutions. One study[5] identifies factors affecting an individual's exposure from a hand-held source within a walk in spray booth. These factors include; 1) the mass flow of the pollutant, 2) the source configuration and momentum, 3) the hood air flow, 4) the position of the worker and source with respect to the hood, 5) activity level of the worker, 6) air supply configuration, and 7) thermal factors.

By holding factors 1, 2, 5, 6, and 7 constant, it is possible to observe the effects of worker position and hood air flow rate on the concentration of contaminant in the breathing zone of the worker. These two factors may be the easiest to control and may have the most significant effect on breathing zone concentration.

In a walk-in spray booth, the worker is normally positioned upstream with the source (spray gun) between the worker and the object (i.e. box). In this orientation, the worker's body becomes an obstruction in the flow field resulting in reverse flow and turbulent mixing immediately downstream of the worker. If the source of contamination is located within this zone, it can be drawn back toward the worker and into the breathing zone.(7)

Normally, as a vortex forms around a single obstruction, it grows, then separates from the surface of the obstruction and moves downstream.(10) However, if an additional obstruction is placed downstream of the contaminant source (i.e. a box) the vortex shedding is disturbed since air movement downstream is blocked. Streamlines around the second obstruction must be followed, and may provide additional opportunity for the contaminant to enter the breathing zone as it is re-entrained into the backflowing eddy due to boundary layer separation effects from the worker's body.

It is possible to observe the interactions of air flow around a worker or object and the contaminant movement to the worker's breathing zone. Earlier studies addressed simpler models in an attempt to develop better computational representations of contamination transport. Authors(5) examined the phenomenon of boundary layer separation on local exhaust design, as well as factors affecting design of non-enclosed LEV on control of a hand held source.(6) Later, airflow patterns were examined around a worker in a uniform free stream and worker exposure from a hand held source was modeled with empirical equations.(8,9) It has also been noted that when an object of finite height is present in a free flow steam, there is a significant downwash effect from the free end, where air flows down over the top of the object.(11)

Airflow from the side as opposed to from the back has also been investigated. Authors(6) note that with non-enclosed LEV, positioning the worker 90° to the direction of airflow results in a statistically significant decrease in breathing zone concentration compared to the typical orientation with the source between the body and the exhaust system.

The purpose of this research is to investigate the effect of worker position, relative to object, on the breathing zone concentration of a contaminant generated from a hand-held source. Significant reduction in breathing zone level of contaminant is expected when a worker is positioned with airflow to the side and increased airflow should reduce the breathing zone concentration as well.

THEORY

As described earlier, when fluid flows past a blunt object, a boundary layer forms on the surface of the object.(5) The boundary layer is the region that extends from the surface, where the velocity is zero, to a point some distance from the surface where the velocity is 99% of the free stream value.(12) Air flowing around an obstacle accelerates on the upstream side of the object and decelerates on the downstream side. This results in reverse flow on the downstream side due to the presence of an adverse pressure gradient. A vortex forms on the downstream side which can carry contaminant upstream into the breathing zone. If no other obstructions are present, the vortex grows in size, separates from the object and moves downstream. The frequency of vortex shedding is a function of air velocity and object size (or Reynolds number).

A simple conceptual model was offered based on treating the worker as a two dimensional cylinder with vortex shedding as the principle contaminant removal mechanism.(5) A recirculation zone is assumed to exist downstream of the worker and a point source of contamination is released into the zone. For this model the average steady-state concentration (C_{st}) within the zone is

$$C_{st} = \frac{Q_s}{Q_v} \tag{1}$$

where Q_S = the flow of contaminant into zone and Q_V is the air-contaminant-mixture flow out of the zone. Here, the formation zone is assumed to be a cylinder of equal height (H) and width (D) as a worker. The volume cleared by each vortex shedding event is assumed to be one-half the formation region, thus the vortex volume (V) is

$$V = \frac{\pi}{8} D^2 H \tag{2}$$

The frequency with which vortices are shed is

$$f = \frac{0.21U}{D} \tag{3}$$

where f is the frequency of vortex shedding, U is the velocity of the fluid stream and 0.21 is the Strouhal number which remains relatively constant for Reynolds numbers from 400 to about 200,000.(13)

Since the frequency in Equation 3 considers only one side of the cylinder, the total frequency will be twice this value or $2f$. This leads to a simple approximation for the average concentration.

$$C_{st} = \frac{Q_S}{Q_V} = \frac{19Q_S}{\pi UHD} \tag{4}$$

This original mass balance model was later revised based on data collected during a study examining the 3-dimensional effects of a mannequin substituted for the cylinder.(8) Visual observation showed that smoke below the hip level moved downward into a lower reverse flow region and thus escaped entrainment into the vortex crossing into the breathing zone. Also, a vortex shedding frequency corresponding to an average Strouhal number of 0.19 was observed between the chest and hip level (approximately 0.3H). Accordingly, the vortex volume (V) was adjusted to

$$V = 0.7\left[\frac{\pi}{4} D^2\right](0.3H) \tag{5}$$

and the frequency adjusted to

$$f = \frac{0.19U}{D} \tag{6}$$

The modified approximation for the spatially and temporally averaged concentration is

$$C_{st} = \frac{50Q_S}{\pi UHD} \tag{7}$$

Experimental data, showed Equation 7 overestimates the observed average concentration. Statistical analysis of the data led to empirical formulas for the spatially and temporally averaged concentration, C_{st} (concentration in the reverse flow region), and for the concentration observed in the breathing zone, C_{bz}.[8]

$$C_{st} = \frac{10.96Q_s}{UHD} \quad (8)$$

$$C_{bz} = \frac{8.62Q_s}{UHD} \quad (9)$$

Equation 9 is used in this work for comparison of average breathing zone concentrations for the same worker position, but including an additional obstruction to the free field flow in the booth (e.g. a box).

Finally, a study was conducted[9] with a full-size walk in spray booth, varying: 1) the momentum of the source; 2) the presence of an obstacle in front of the worker (e.g. a flat plate); 3) the movement of the worker to simulate painting motion; and 4) the distance between the worker and the outlet of the spray gun (tracer gas was used in the spray gun, instead of paint). The results showed the most significant impact on breathing zone concentration was the outlet velocity of the spray gun pointed downstream.

The same study observed that with higher source flows, lower free stream velocity resulted in slightly lower breathing zone concentrations than did higher free stream velocities in the booth. But when the source flow was negligible, the lower free stream velocity resulted in slightly higher breathing zone concentrations than did higher free stream velocities. In addition, the breathing zone concentration was generally reduced by one-half when the flat plate was placed in front of the worker (downstream). This study also found Equation 9 to agree well with experimental data collected in the full-size spray booth under the conditions which matched the underlying assumptions governing the equation.

MATERIALS AND METHODS

General

The experiment was carried out in a low speed, open circuit wind tunnel 1.52 m square and 2.44 m deep (5 ft X 5 ft X 8 ft) with velocity range of 0.127-1.40 m/s (25-275 fpm). The entrance of the wind tunnel is equipped with a flared flange and the rear wall consists of a pegboard with .064 cm (.024 in.) holes to create a perforated plenum to provide better air distribution across the tunnel (See Figure 1).

Air velocities determined though calibration data from previous experiments were verified with a calibrated hot-wire anemometer. Observation windows on one side and top of the wind tunnel were used for flow visualization.

Configuration A (see Figure 2) will represent a worker in the traditional position (air flow from behind the worker with the source between the worker and the work). Configuration B will orient the worker 90° to the direction of the air flow (sideways to the airflow and to the side of the object with the source between the worker and the work).

Additionally, the 3-dimensional effects of the worker and object were evaluated. Configurations A and B will substitute a floor-to-ceiling elliptical cylinder 1.52 m (5 ft) tall to represent the worker and a floor-to-ceiling box to represent the work. This had the affect of creating a 2-dimensional model of air flow for comparison to a 3-dimensional model using the mannequin.

For the wind-tunnel tests, a commercial anthropometric mannequin, 1.04 m tall (41 in.) tall and 20 cm (8 in.) wide at the chest was placed at the centerline of the tunnel. A wooden box, 0.41 m (16 in.) square and 1.12 m (44 in.) tall was placed roughly arm's length away 25 cm (10 in.) downstream to represented the work.

A neutrally buoyant mixture consisting of 10.0% sulfur hexafluoride, 45.8% helium and 44.2% air was used as a tracer gas. The mixture was released through a 1/4 in. diameter ceramic sphere at a rate of 220-230 cc/min. (0.0008 cfm of pure SF_6, 0.0036 cfm of air and 0.0037 cfm helium) as measured with an in-line DuPont mini-Buck calibrator. Pores in the sphere allow the gas to diffuse in all directions.

The source of the contaminant was placed between the mannequin and the box at chest level in the mannequin's hands at a height of 79 cm (31 in.) and a distance from the box of 15 cm (6 in.) to simulate normal work orientation. With the cylinder, the ceramic sphere was positioned halfway between the cylinder and the object, at the same level as the sampling point (79 cm.).

An electron capture detector (ECD) was used to measure SF_6 tracer gas. A sampling tube was connected from the mannequin's mouth through the back of the head and connected to the sampling port to the detector nozzle. Air was continuously drawn through the mannequin's mouth throughout the sampling period.

Experiments were carried out in free stream air velocities of 100, 150 and 250 fpm The Reynolds numbers associated with these velocities are 6837, 10256 and 17092, respectively, based on a mannequin width of 20 cm (8 in.). The system was allowed to equilibrate for approximately 5 min. before data were gathered.

Two blocks of three to six trials were conducted for each configuration at each of three airflows (100, 150, 250 fpm). Each trial consisted of approximately 100 data points collected by noting the ECD display at 5 second intervals. For each configuration and airflow, the trials were combined into one data set of 300-600 points. For each configuration, the experiment was repeated once on a separate day to assure reproducibility of results.

Flow Visualization

Smoke generation techniques introduced[14,15] and later refined,[7] were used to visualize airflow around the worker and object. Several strands of 0.01 inch NiCr wire were twisted together and strung across the sampling region passing through the point of contaminant release (just above the hands of the mannequin; 5 inches from the sampling point of the cylinder). The wire was held taught by springs at each end of the wire. A variable DC power source was connected to each end of the wire to provide current to the wire which heated the smoke-generating oil. Paraffin oil was spread onto the wire with a paintbrush and when a current of 25 volts was passed through the wire, a dense, white smoke was produced for periods of 20-40 seconds in the horizontal plane of airflow. Some lofting of the smoke was observed, but this was less pronounced at higher air flows. Photographs were obtained through the windows in the side and top of the wind tunnel.

RESULTS AND DISCUSSION

Data Analysis

Probability plots of the raw data showed no linear preference for a log transformation. The data were analyzed assuming a normal distribution and observed data were transformed into true SF_6 concentrations using calibration curves for the ECD. Average values for each data set were determined from the frequency distribution. This resulted in 24 data sets; one for each configuration (2), airflow (3), dimension (2), and block (2). Table 1 shows the experimental data divided into blocks. Table 1 format was used for statistical analysis.

Table 2 combines the means of the two blocks to obtain one overall mean for each condition. This was done by taking the mean of Block 1 times the number of data points in Block 1 plus the mean of Block 2 times the number of data points in Block 2 all divided by the total number of data points. The overall mean is the observed value in comparisons to calculated values.

Configuration A (airflow from the back) showed dramatically higher breathing zone concentrations than Configuration B (airflow from the side). Table 2 shows that orienting the mannequin sideways to the airstream (as opposed to airflow from the back) resulted a reduction of breathing zone concentration of 187-fold at 100 fpm freestream velocity, 994-fold at 150 fpm, and 137-fold at 250 fpm for the mannequin. Reductions of 384-fold at 100 fpm , 580-fold at 150 fpm, and 436-fold at 250 fpm freestream velocity were measured for the cylinder. The difference is illustrated in Figure 3.

Figures 4 and 5 illustrate the mean breathing zone concentration of SF_6 for the mannequin and the cylinder for Configurations A and B at the different flow rates. In Configuration A, the ratio of mannequin breathing zone concentration to cylinder breathing zone concentration for 100, 150 and 250 fpm freefield airflow is 0.85, 0.56, and 0.38, respectively. This shows a consistent decrease in breathing zone concentration for the mannequin versus the cylinder. This may be accounted for by the increased distance between the source and the mouth of the mannequin, allowing for additional mixing with room air in the backflow region and additional time to shed the contaminant. For the cylinder, the sampling point is located on the downstream surface of the cylinder at the same height as the contaminant release point. An earlier study shows that the reverse flow region is narrower at the neck of the mannequin than at chest level and varies with the width of the mannequin.(7) This change in reverse flow region may also account for the lower concentration observed at the mouth than at chest level.

In Configuration B, the ratio of SF_6 concentration at the breathing zone of the mannequin to the sampling point of the cylinder for 100, 150 and 250 fpm freefield airflow is 1.74, 0.32, and 1.19, respectively. The trend is inconsistent with findings for Configuration A, but since the calculated average concentrations are near the limit of detection for the experiment (0.1 ppm), it is questionable if these values are comparable. Nonetheless, the breathing zone concentrations were found to average < 1 ppm for all data sets in Configuration B.

Observed breathing zone concentrations for Configuration A were compared to those values predicted by Equations 4 (C_{st}), 7 (C_{st}) and 9 (C_{bz}) and are shown in Table 3. Figure 6 shows the relationship between these equations and observed values. Recall that equations 4 and 7 are approximations for concentrations of spatially and temporally averaged values for the entire reverse flow region and Equation 9 an approximation for the average breathing zone concentration. All three equations refer to a single cylinder in a free flow field and do not take into account the additional object (i.e. a box). The observed values for Configuration A are higher, on average, than any of the equations. Observed values for the cylinder were higher than those for the mannequin. Observed values were closest to values predicted by Equation 7.

Comparison of observed values to those predicted by Equation 9 revealed ratios of 2.5, 2.4. and 1.4 to 1 for observed to predicted breathing zone concentration. This may be interpreted as roughly a 2:1 greater breathing zone concentration for Configuration A as opposed to a mannequin in free stream with no additional object. These observations appear to contradict work by Kim[9] who showed that breathing zone concentrations actually dropped by a factor of 2-3 when a plate was placed downstream of the worker. However, the "negligible" momentum of the contaminant source in his experiment (0.015 cfm) was at least 18.5 times greater than in this study (0.00081cfm), since the volume was 18.5 times greater and directed downstream. The momentum of the source may play a role in Kim's experiment to lower breathing zone concentration. Another possibility is that the flow streams around flat plates differ from those around a solid box and could provide different opportunities for the contaminant to avoid being drawn into the reverse flow region.

Statistical Analysis

The data are presented in Table 4 in the format suitable for statistical analysis by ANOVA. Tables 5 and 6 separate the data for the cylinder and mannequin and show the results of an initial ANOVA used to evaluate the individual significance of each factor. Blocking (date of data collection) is not found to be significant at the $p = 0.05$ level for either the cylinder ($p = 0.730$) or the mannequin ($p = 0.645$). A two-way Model I ANOVA is then presented using sulfur hexafluoride concentration as the dependent variable, with flowrate and position as independent variables.

Table 7 shows the results of the two-way ANOVA for the cylinder data. Flow rate is not found to be a significant factor for SF_6 concentration ($p = 0.067$), though it suggests a relationship at a slightly higher level of significance. Position is found to be significant ($p < 0.0005$). Interaction between flowrate and position ($p = 0.069$) is not found to be significant, though interaction is suggested at a higher level of significance.

Table 8 gives the results of the two-way analysis of variance for the mannequin data. Flow rate is a significant factor in breathing zone concentration ($p = 0.002$). Position is also found to be significant ($p < 0.0005$). The interaction between flowrate and position is significant at the $p = 0.002$ level.

Interaction between airflow and position for the mannequin and suggested interaction with the cylinder appears to occur in Configuration A, where higher airflow results in reduced breathing zone concentration. This affect was inconsistent in Configuration B.

Flow Visualization

The results of the flow visualization are shown in the photographs (Figures 7-11) and clearly show the airflow patterns around the mannequin and cylinder in each configuration. Figure 7 uses a vertical smoke-wire 6 inches downstream of the mannequin to produce smoke from the plane of the contaminant release point. The smoke from eye level on down is drawn back toward the mannequin. From eye to chin level, the backwash effect is less pronounced, but below chin level, almost all of the smoke is drawn back to the mannequin's body. The distinct separation of the airflow into an upper region rotating clockwise and a lower region rotation counter-clockwise was not evident as in an earlier study.[7] The area from the top of the head to the nose may be affected by the downwash effect over the top of the mannequin's head.

Figure 8 shows Configuration A for the mannequin with an air flow of 150 fpm. The reverse flow region is again evident, but appears wider than shown in photos of the earlier study.[7] The reverse flow region is again not as well defined as when the object (e.g. box) is not present. At higher airflows the degree of reverse flow seemed to be less, and the eddy patterns were less visible. The width of the reverse flow region is greater than the width of the mannequin, but not as wide as the box.

Figure 9 shows the cylinder at a flow of 150 fpm in Configuration A. The reverse flow pattern is regular and its width is wider than the cylinder, but not as wide as the box. The flow pattern for Figure 7, in comparison, is not as regular, showing the 3-dimensional effects of the variation in mannequin width from chest to mouth. The downwash effect may also interfere with structured eddy formation with the mannequin.

Figure 10 shows the mannequin in Configuration B at a flow of 150 fpm. The air flow lines are distinct and can be seen to flow around the mannequin and box. Not visible in the photograph are the backflow eddies downstream of the mannequin and box, though it is evident that the reverse flow does not travel back to the sampling point or breathing zone. Also, the streamlines past the contaminant source do not seem to be disturbed, and flow from the hand region to the breathing zone is not evident.

Figure 11 shows the cylinder in Configuration B with an airflow of 150 fpm. The streamlines are clearly defined and little disturbance is present before the downstream side of the cylinder.

The roughly two to three orders of magnitude difference in concentration of SF_6 between the two configurations is attributed to reverse flow region formation. As illustrated in Figures 7 and 8 , the reverse flow region for Configuration A includes the contamination release point. This draws the contaminant back toward the mannequin and cylinder. For Configuration B, the reverse flow region still forms, but it is downstream of the worker and work and does not encompass the contaminant release point. Figures 9 and 10 show the smooth streamlines around the mannequin, cylinder and box. The streamlines are straighter at higher airflow rates, with the lower airflow rates allowing some wavering of the airstream.

CONCLUSIONS

Flow visualization techniques and experimental results show worker position relative to air flow plays a significant role in breathing zone concentrations from a hand-held contaminant within a simulated spray booth operation.

Experimental data show a two to three orders of magnitude difference in concentration between the two positions. This difference is attributed to the formation processes of reverse flow regions immediately downstream of the worker and source.

When an object is present, representing a workpiece, it may interfere in the contamination removal methods such as vortex formation and shedding. Distinct reverse flow eddies visible when just the worker and source are present in the freestream do not form as readily when an object is placed downstream. The disturbance caused by an object is less pronounced when the airflow is from the side.

It must be remembered that this experiment represents idealized conditions for the configurations studied. In a real paint booth operation many of the factors held constant in the experiment would vary. Worker motion and source momentum are probably the largest contributors to the limitations of this work. As a worker moves, new reverse flow regions are constantly forming and shedding. This may create eddies which draw contaminant into the worker's breathing zone even while standing perpendicular to airflow.

Another factor found to greatly influence the reentrainment of contaminant into the breathing zone is momentum of the source. In the case of a spray painting operation, the paint and solvent are delivered under pressure. The momentum of the droplets may not follow airflow streams, the impaction of the paint droplets may cause reflection or splattering of the paint, and the air delivered to carry the paint forms new air steams which may overpower the free field.

This study may be more applicable to operations in which little no momentum is imparted onto the source; such as a welding operation or brush painting, where the solvent in the paint evaporates from the surface of the workpiece.

In addition, workpieces are usually not flat, regular shapes. Different objects will create different streamline flows, which may influence breathing zone concentration.

Further study is recommended to examine the effects of object size/shape and source momentum on the breathing zone concentrations.

REFERENCES

1. American Conference of Governmental Industrial Hygienists: Industrial Ventilation — A Manual of Recommended Practice. 20th ed. Cincinnati, Ohio: American Conference of Governmental Industrial Hygienists, 1988.

2. White, F.M.: Fluid Mechanics, 2nd ed. McGraw-Hill Book Company, New York (1986).

3. Ljungqvist, B.: Some Observations on the Interaction Between Air Movements and the Dispersion of Pollution. Document D8. Swedish Council for Building Research, Stockholm (1979).

4. Ljungqvist, B. and B. Reinmüller: Interaction Between Air Movements and the Dispersion of Contaminants. Clean Zones with Unidirectional Air Flow. Proceedings of the International Congress. Basel, Switzerland, (1992)

5. George, D.K., M.R. Flynn and R. Goodman: The Impact of Boundary Layer Separation of Local Exhaust Design and Worker Exposure. Appl. Occup. and Environ. Hyg., 5:501-509 (1990).

6. Flynn, M.R. and W.K. Shelton: Factors Affecting the Design of Local Exhaust Ventilation for the Control of Contaminants from Hand-Held sources. Appl. Occup. and Environ. Hyg., 5:707-714 (1990).

7. Kim, T.H. and M.R Flynn: Airflow Pattern around a Worker in a Uniform freestream. Am. Ind. Hyg. Assoc. J. 52(7):287-296 (1991).

8. Kim, T.H. and M.R Flynn: Modeling a Worker's Exposure from a Hand-Held source in a Uniform Freestream. Am. Ind. Hyg. Assoc., J. 52 (11):458-463 (1991).

REFERENCES (CONTINUED)

9. Kim, T.H. and M.R Flynn: The Effect of Contaminant Source Momentum on a Worker's Breathing Zone Concentration in a Uniform Freestream. Am. Ind. Hyg. Assoc. J. 53(12):757-766 (1992).

10. Burgess, W.A.; M.J. Ellenbecker; R.D. Treitman: Ventilation for Control of the Work Environment. John Wiley & Sons Inc., New York (19891).

11. Kawamura, T., M. Hiwada, T. Hibino, I. Mabuchi, and M. Kumada: Flow Around a Finite Circular Cylinder on a Flat Plate. Bull. Jpn. Soc. Mech. Eng. 27(232):2142-2151 (1984).

12. Flynn, M.R., C.T. Miller, M.L. Fitzgerald, D.K. George, K.N. Smith, and K.D. Tum Suden. The Simulation of Local Exhaust Ventilation Problems. The Ann. of Occ. Hyg. Ventilation '88, Proceedings of the Second International Symposium on Ventilation for Contaminant Control, London (1988).

13. Roshko, A.: On the Development of Turbulent Wakes from Vortex Streets. NACA Report 1191 (1954).

14 Goldstein, R.J., ed.: Fluid Mechanics Measurements. 1st ed. New York: Hemisphere Publishing Company, 1983. pp. 331-334.

15 Tsanis, I.K.: "Flow Visualization in Circulation Air Flows Using the Smoke-Wire Technique." Paper presented at the Fourth International Symposium on Flow Visualization, Paris, August 1986.

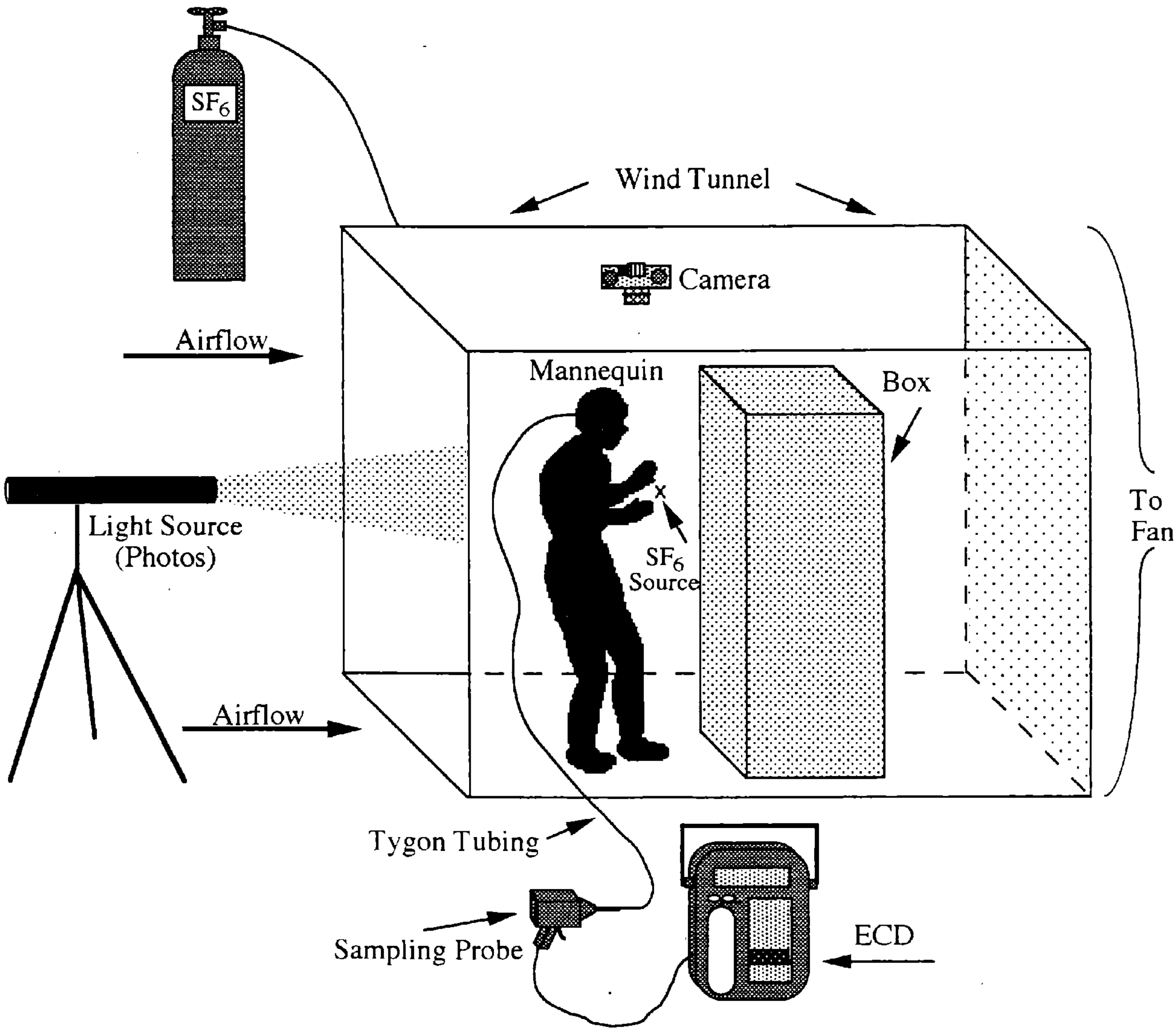

Figure 1. Schematic of Testing Facility

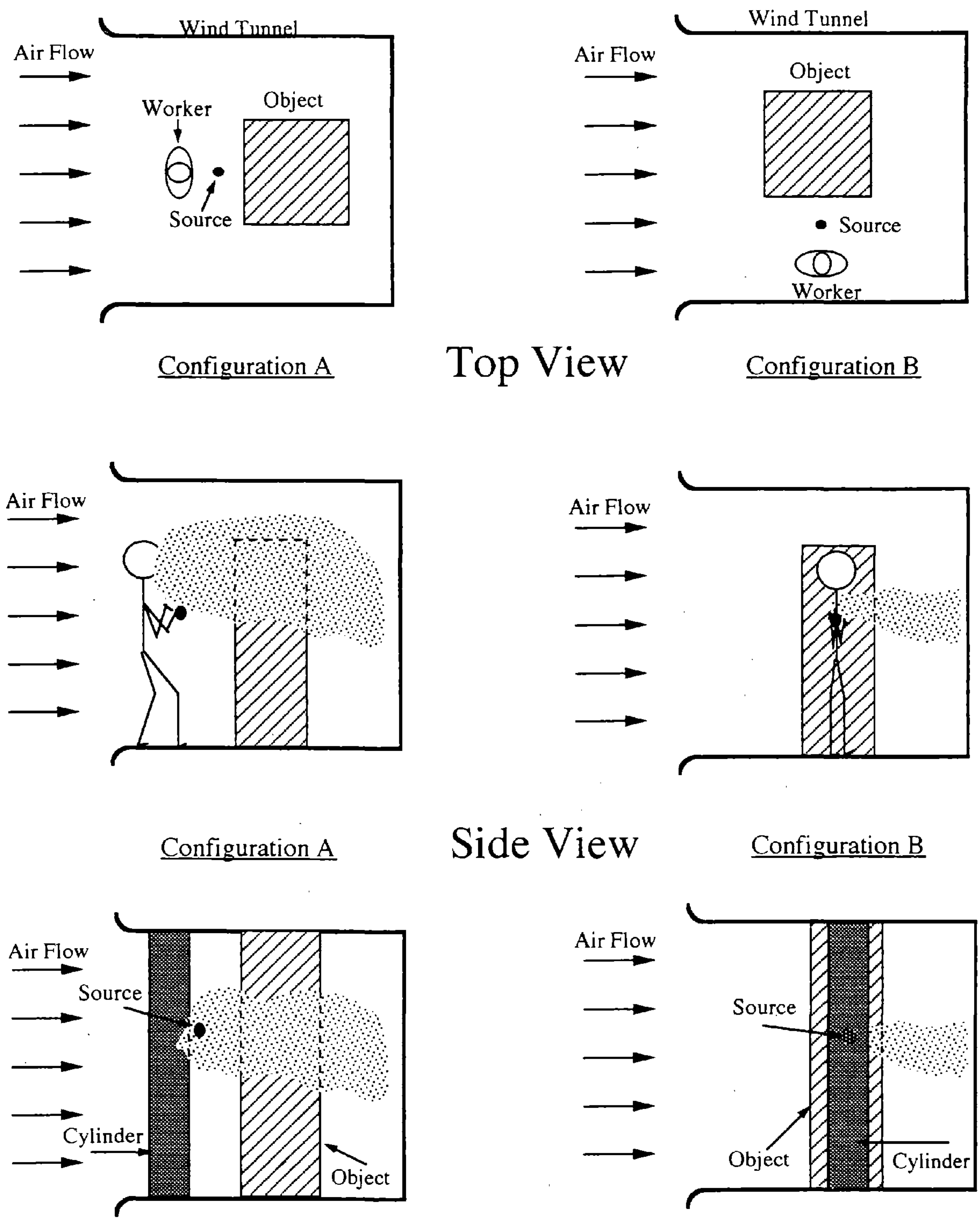

Figure 2. Configurations A & B

Figure 3. Comparison of Mannequin and Cylinder, Configuration A

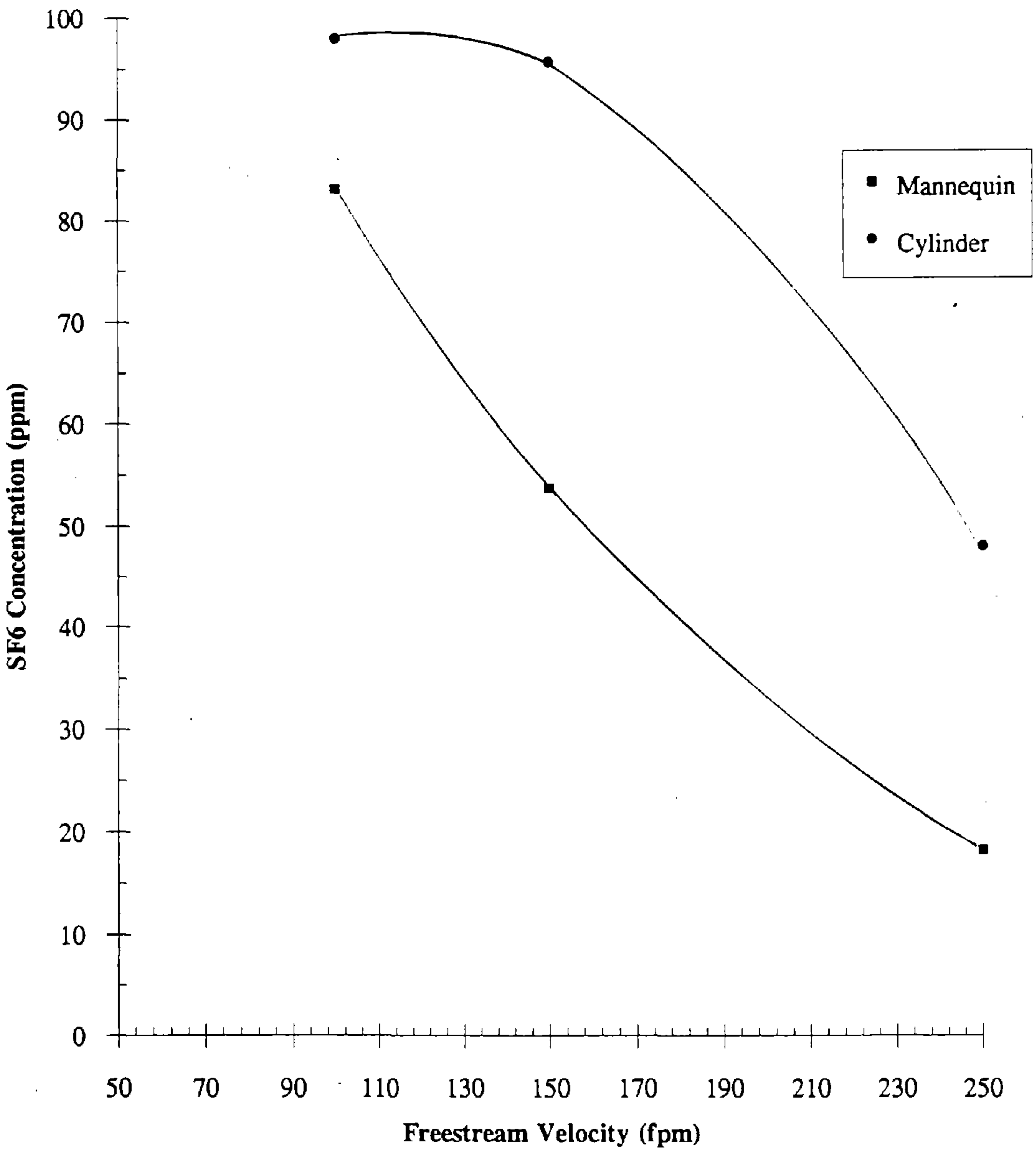

Figure 4. Comparison of Mannequin and Cylinder, Configuration B

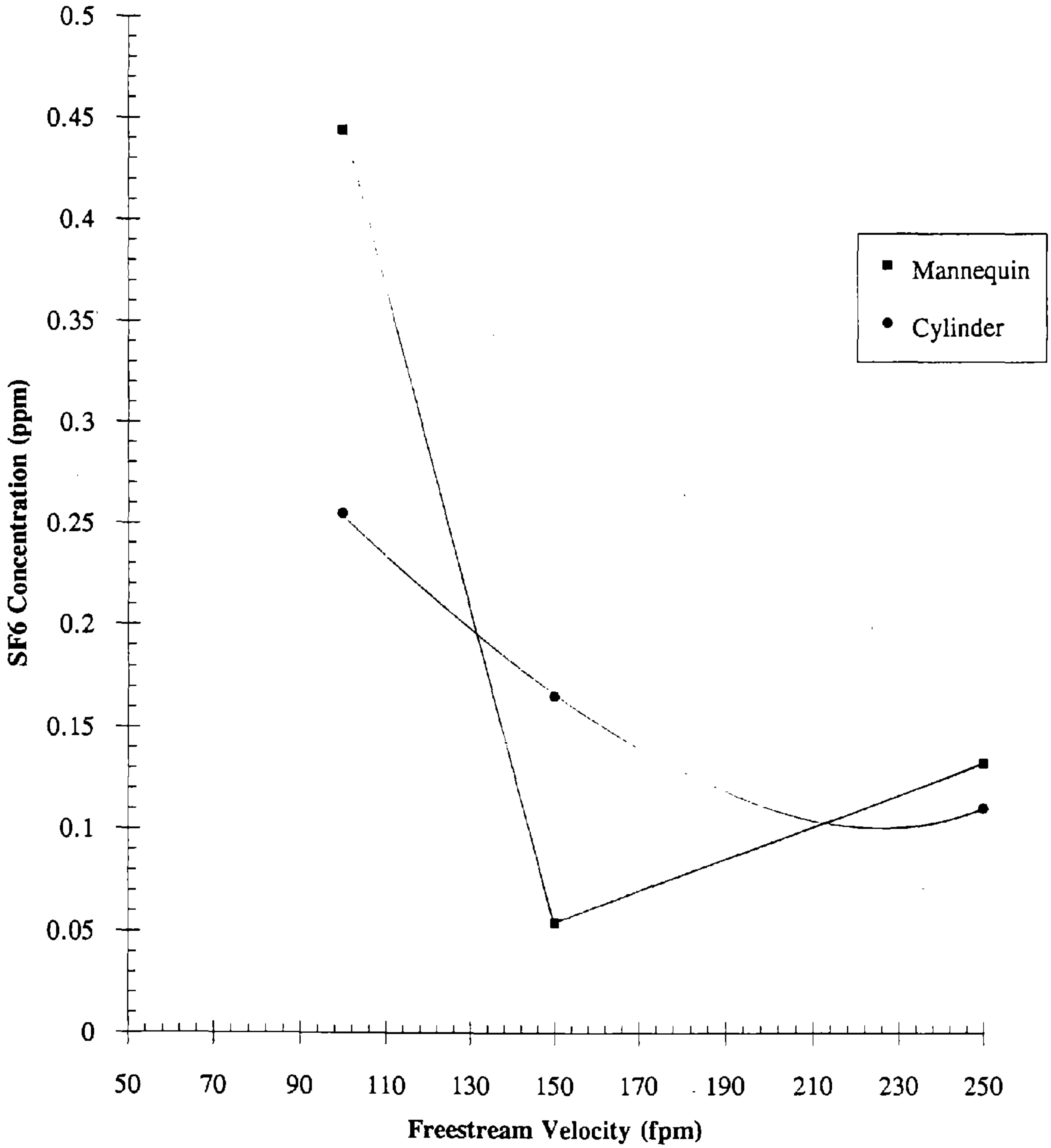

Figure 5. Comparison of Mannequin and Cylinder, Configurations A & B

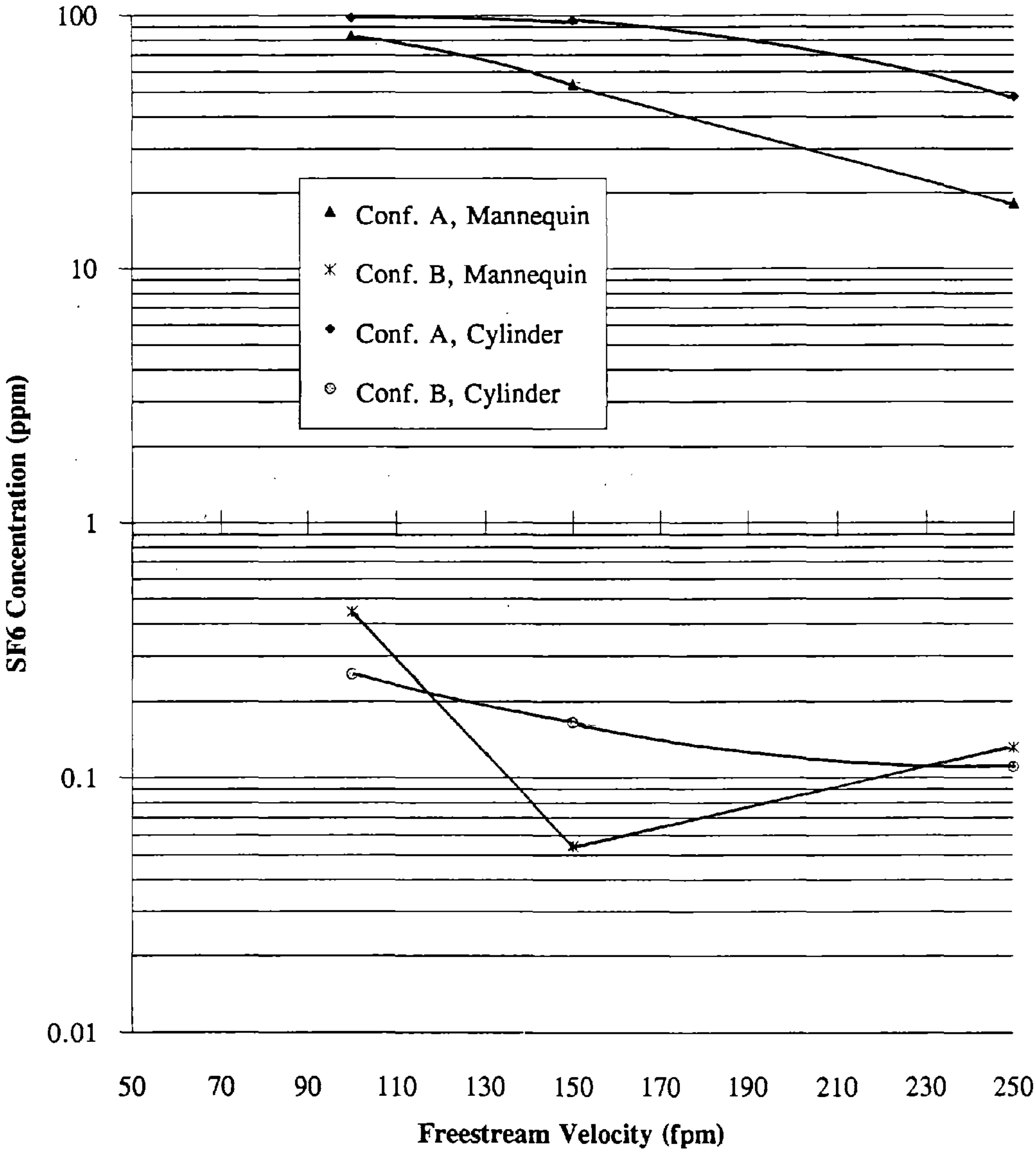

Figure 6. Comparison of Observed Results vs. Calculated

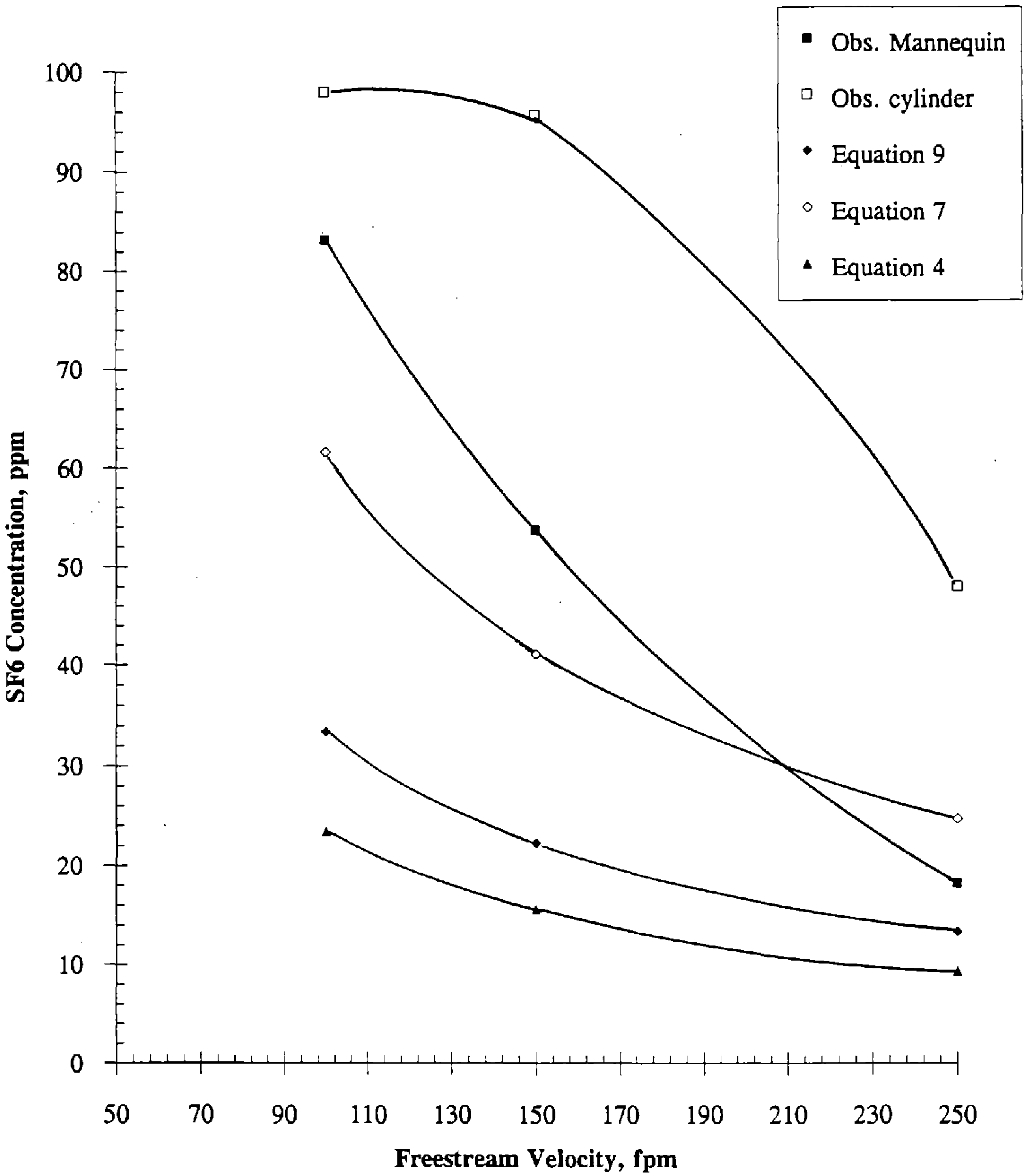

Table 1. SF6 Concentration (ppm), 2 Blocks

	Freestream Airflow (fpm)					
	100	*150*	*250*	*100*	*150*	*250*
	93.0	50.0	19.0	107.0	96.0	71.0
Configuration A	70.0	57.6	17.5	89.0	95.5	30.6
Configuration B	0.779	0.052	0.189	0.320	0.193	0.082
	0.100	0.055	0.097	0.190	0.148	0.126
	Mannequin			*Cylinder*		

Table 2. Combined Mean SF6 Concentration (ppm)

	Freestream Airflow (fpm)					
	100	*150*	*250*	*100*	*150*	*250*
Configuration A	83.2	53.7	18.2	98.0	95.7	48.0
Configuration B	0.444	0.054	0.132	0.255	0.165	0.110
	Mannequin			*Cylinder*		

Table 3. Observed and Calculated Breathing Zone Concentrations (ppm SF6), for Configuration A

Velocity (fpm)	Observed (ppm) Mann.	Cyl.	Equation 9 Cbz=(8.62 Qs)/UHD Kim, revised	Equation 7 Cst=(50 Qs)/PI*UHD Kim, original	Equation 4 Cst=(19 Qs)/PI*UHD George,et al
100	83.2	98.0	33.4	61.6	23.4
150	53.7	95.7	22.2	41.1	15.6
250	18.2	48.0	13.3	24.6	9.4

Table 4. Raw Data as Arranged for ANOVA

Conc.: mean concentration of sulfur hexafluoride
Flow Rate: 1 = 100 fpm; 2 = 150 fpm; 3 = 250 fpm
Position: 1 = Configuration A; 2 = Configuration B
Block: 1 & 2 collected on different days
Dimension: 1 = Cylinder; 2 = Mannequin

Conc. (ppm)	*Flow Rate*	*Position*	*Block*	*Dimension*
107	1	1	1	1
89	1	1	2	1
96	2	1	2	1
95.5	2	1	1	1
71	3	1	2	1
30.6	3	1	1	1
0.32	1	2	1	1
0.19	1	2	2	1
0.193	2	2	2	1
0.148	2	2	1	1
0.082	3	2	2	1
0.126	3	2	1	1
93	1	1	1	2
70	1	1	2	2
50	2	1	2	2
57.6	2	1	1	2
19	3	1	2	2
17.5	3	1	1	2
0.779	1	2	1	2
0.1	1	2	2	2
0.052	2	2	2	2
0.055	2	2	1	2
0.189	3	2	2	2
0.097	3	2	1	2

Table 5. Analysis of Cylinder Data for SF6 Concentration

Source	*Sum-of-squares*	*DF*	*Mean-square*	*F-ratio*	*P*
FLOWRATE	1424.684	2	712.400	2.126	0.190
POSITION	19848.668	1	19848.668	59.226	0.000
BLOCK	43.210	1	43.210	0.018	0.895
Error	2345.950	7	335.140		

Table 6. Analysis of Mannequin Data for SF6 Concentration

Source	*Sum-of-squares*	*DF*	*Mean-square*	*F-ratio*	*P*
FLOWRATE	2028.143	2	1014.071	3.206	0.103
POSITION	7794.225	1	7794.225	24.638	0.002
BLOCK	73.456	1	73.456	0.232	0.645
Error	2214.408	7	316.344		

Table 7. Two-way Analysis of Variance, Cylinder

Dep var: CONC N: 12 Multiple R: .979 Squared multiple R: .959

Source	*Sum-of-squares*	*DF*	*Mean-square*	*F-ratio*	*P*
FLOWRATE	1424.684	2	712.342	4.369	0.067
POSITION	19848.668	1	19948.668	121.744	0.000
FLOWRATE* POSITION	1410.942	2	705.471	4.327	0.069
Error	978.215	6	163.036		

Table 8. Two-way Analysis of Variance, Mannequin

Dep var: CONC N: 12 Multiple R: .988 Squared multiple R: .976

Source	*Sum-of-squares*	*DF*	*Mean-square*	*F-ratio*	*P*
FLOWRATE	2028.143	2	1014.071	20.643	0.002
POSITION	7794.225	1	7794.225	158.667	0.000
FLOWRATE* POSITION	1993.124	2	996.562	20.287	0.002
Error	294.74	6	49.123		

Figure 7. Configuration A, Mannequin, Side View

Figure 8. Configuration A, Mannequin, Top View

Figure 9. Configuration A, Cylinder, Top View

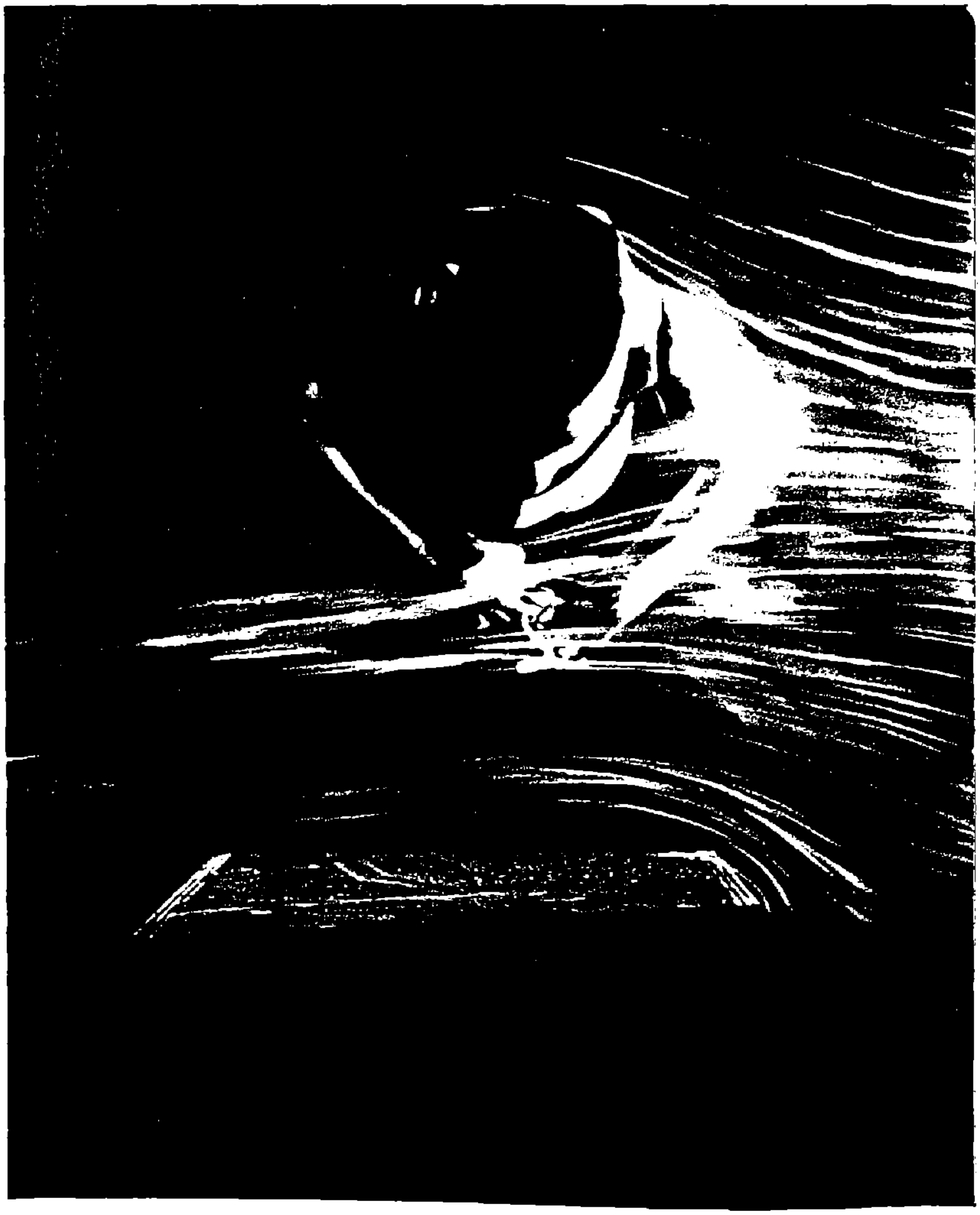

Figure 10. Configuration B, Mannequin, Top View

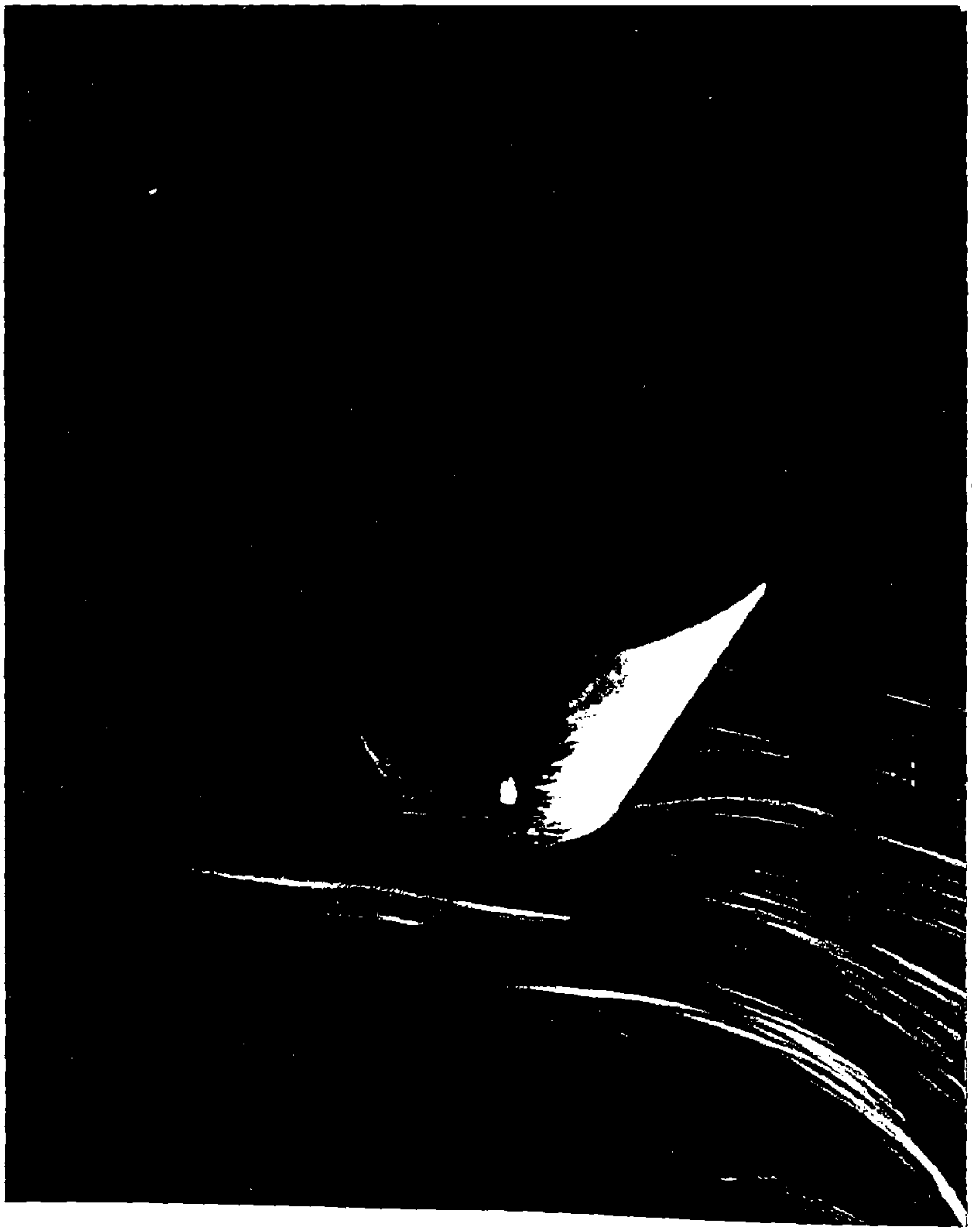

Figure 11. Configuration B, Cylinder, Top View

Figure 12. Calibration Curve for 5/24/93, "L" Sinter

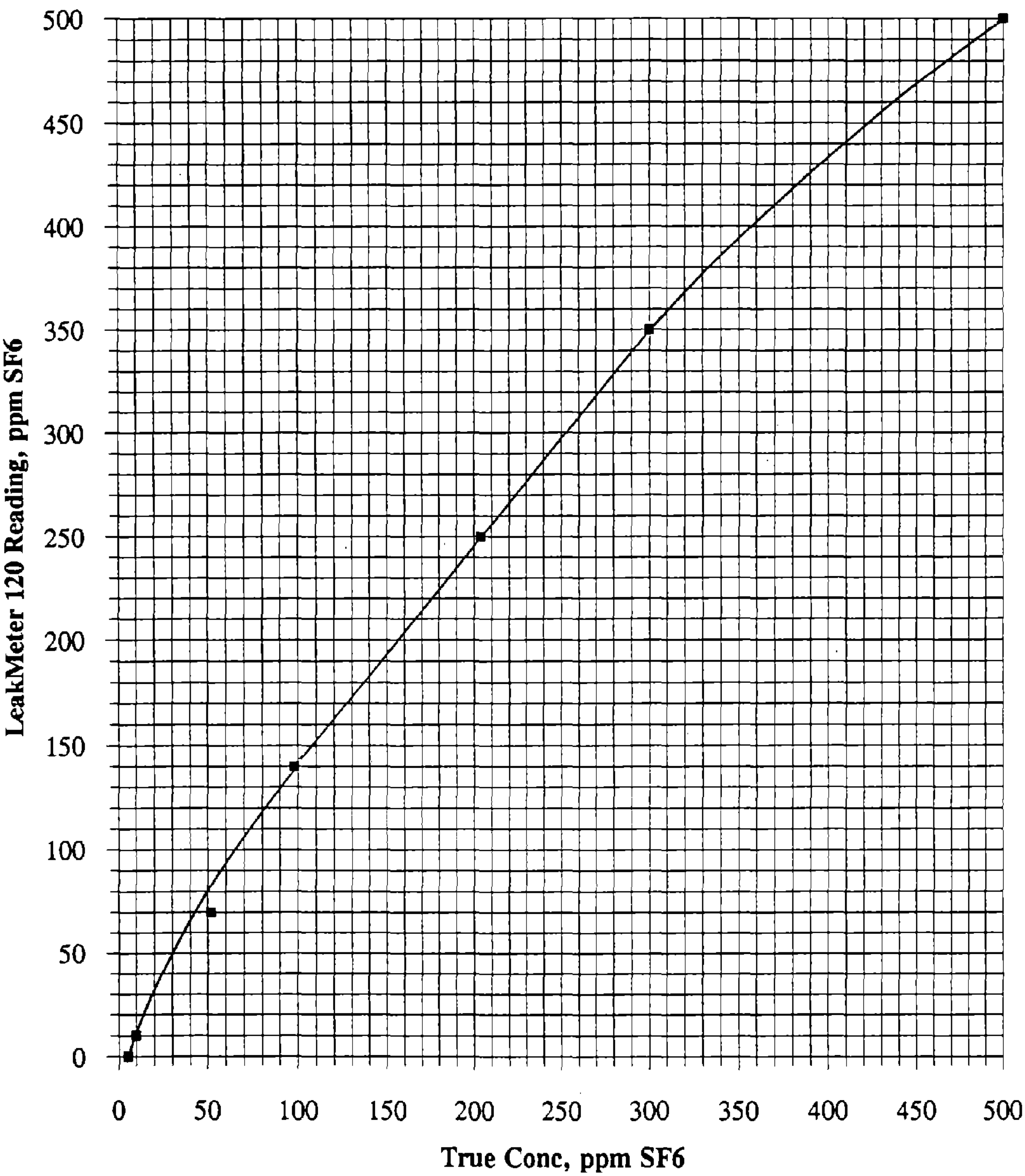

Figure 13. Calibration Curve for 6/2/93, 6/4/93, "L" Sinter

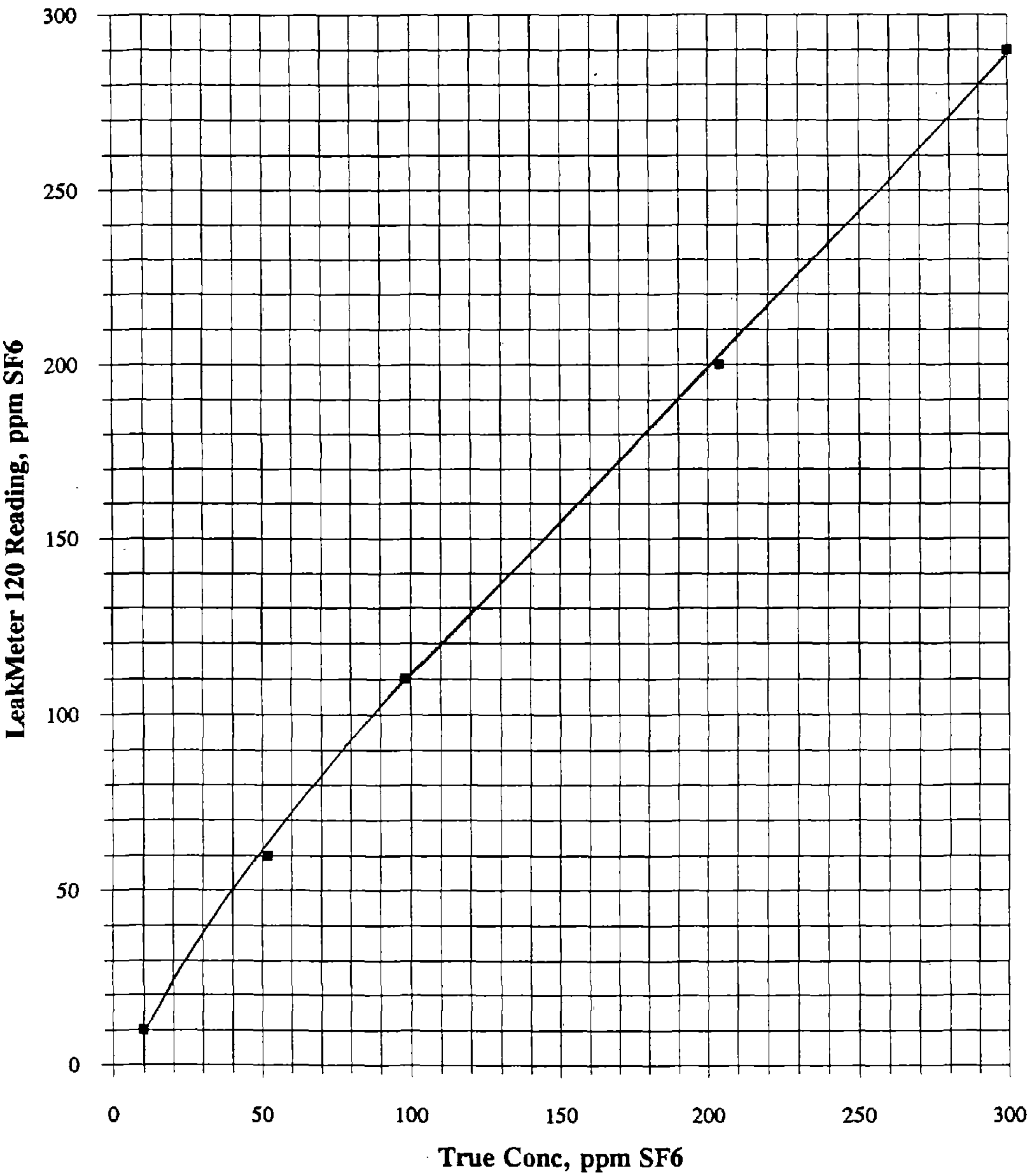

Figure 14. Calibration Curve for 6/4/93, "H" Sinter

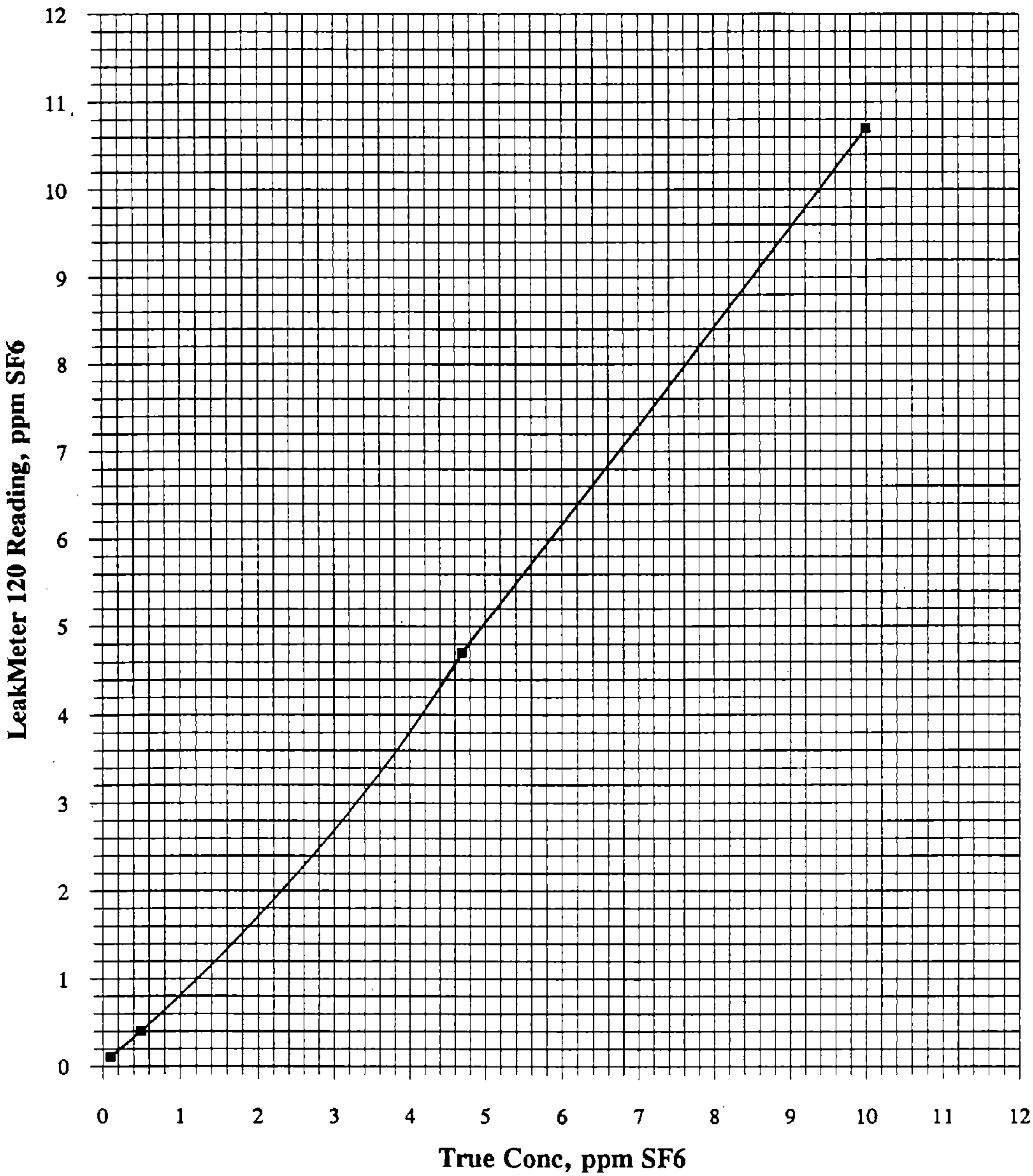

Figure 15. Calibration Curve for 5/25/93, 6/2/93, 6/4/93, "H" Sinter